Available online at www.sciencedirect.com

ScienceDirect

Journal of the European Ceramic Society 35 (2015) 1021–1030

www.elsevier.com/locate/jeurceramsoc

Processing of porous mullite ceramics using novel routes by starch consolidation casting

M.H. Talou *, M.A. Camerucci

Ceramics Division, Research Institute for Materials Science and Technology (INTEMA), CONICET/UNMdP, Av. Juan B. Justo 4302, B7608FDQ Mar del Plata, Argentina

Received 25 September 2014; accepted 13 October 2014
Available online 25 October 2014

Abstract

In this article, the development and characterization of porous mullite bodies prepared using two novel forming routes with native starches were studied with the aim of developing bodies without deformation and with homogeneous porous microstructures. Mullite–starch suspensions specific for each route were prepared by mixing and characterized by measuring viscosity. Mullite green bodies were fabricated by heating the suspensions in metallic molds and by burning out the starch, while final porous materials were obtained by sintering at different temperatures. Bodies obtained before and after the burning-out process, and sintered disks, were characterized with porosity measurements and microstructural analysis by SEM. The phases generated after the sintering process were determined by XRD, and pore size distributions were studied by Hg-porosimetry. The obtained results showed that the use of both routes allowed the shaping of homogeneous mullite bodies without causing cracks or deformations and the consequent development of controlled porous mullite microstructures.

Keywords: Starch consolidation casting method; Mullite; Microstructure; Porous ceramics

1. Introduction

In recent years, much attention has been focused on porous ceramic materials due to their wide range of technological applications as thermal insulators, catalyst supports, bioceramics, filters and combustion burners, among others. These materials exhibit several specific properties, such as low density, low specific heat, low thermal conductivity, high surface area and high permeability, which are required for such uses. When they are used for thermal insulation, the materials have to contain a large pore volume fraction, namely high porosity. In particular, porous mullite ($3Al_2O_3{\cdot}2SiO_2$) materials are suitable as thermal insulators because of their low thermal conductivity, moderate thermal expansion coefficient, good chemical durability, and excellent mechanical properties at high temperature.[1–4]

Several processing methods, in particular those based on the direct consolidation of ceramic suspensions into non-porous molds, have been developed with the purpose of preparing porous ceramics. Among them, a non-contaminating low-cost consolidation technique called 'starch consolidation casting' (SCC) has become one of the most popular processing routes for porous ceramics.[5,6] In this method, the starch is used as a body-forming agent of the ceramic suspension when the system is heated between 50 and 85 °C, and as a pore former at high temperature after burning. When the aqueous ceramic–starch suspension is heated, the starch granules swell by water absorption, decreasing the available free water. Thus, the ceramic particles, usually of smaller size than the starch granules, are pressed together in the interstitial space to consolidate into a solid body. After calcination and sintering treatments, a porous material is obtained whose porosity, which is associated with highly interconnected open pores, depends on the amount, shape and size of the swollen starch granules.

In the first reported investigations concerning this forming method,[5,6] the use of native starches as a body-forming agent was not recommended because highly deformed green bodies were obtained. Furthermore, the most satisfactory results were achieved when chemically or physically modified starches

* Corresponding author. Tel.: +54 223 4816600; fax: +54 223 4810046.
E-mail address: mtalou@fi.mdp.edu.ar (M.H. Talou).

http://dx.doi.org/10.1016/j.jeurceramsoc.2014.10.011
0955-2219/

were used.[5–8] Recently, we have reported[8] that the use of a small amount of cold-water-soluble starches (physically modified starch whose granules have the ability to instantly swell in water at room temperature) made the shaping of homogeneous mullite bodies without cracks or deformations possible along with the development of controlled porous microstructures. In addition, we have studied the feasibility of preparing high-quality ceramic green bodies by introducing some other modifications into the conventional route of processing.[9]

Due to the problems associated with using native starches to form ceramics by direct consolidation, two alternative forming routes for aqueous mullite–native starch suspensions are studied in this paper with the aim of developing green bodies without deformation and with homogeneous porous microstructures.

2. Experimental description

2.1. Raw materials

A high-purity commercial mullite powder (MULSM, Baikowski, Charlotte, NC) was used as the ceramic raw material (the alkaline impurity level was less than 0.2 wt%). Excess alumina with respect to the stoichiometric composition (Al_2O_3 = 71.8 wt%, SiO_2 = 28.2 wt%) was determined by inductively coupled plasma atomic emission spectroscopy (ICP-AES). Mullite 3/2 (JCPDS File 74-2419) as the primary phase, and α-alumina (JCPDS File 82-1399), θ-alumina (JCPDS File 11-0517), and cristobalite (JCPDS File 77-1317) as secondary phases, were identified by X-ray diffraction (XRD; X'Pert PRO, PANalytical, Almelo, the Netherlands; radiation of CuKα at 40 mA and 40 kV) (pattern diffraction is included in Fig. 3). In addition, a low-intensity band was also observed in the zone of the more intense diffraction peaks of silica polymorphs (20–30°2θ), which is associated with noncrystalline silicate phases. The mullite powder presented a medium crystallinity that was associated in part with the presence of narrow- and medium-height diffraction peaks when compared to the characteristic peaks of diffractograms of highly crystalline commercial mullite powders.[10] The powder density (3.07 g/cm^3) measured by He-pycnometry (Multipycnometer, Quantachrome Instruments, Boynton Beach, FL, USA) was lower than the theoretical densities of mullite (3.16 g/cm^3), α-Al_2O_3 (3.98 g/cm^3), and θ-alumina (3.28 g/cm^3) due to the contribution of cristobalite (2.3 g/cm^3) and noncrystalline silicate phases (~2.2 g/cm^3).

Considering these results, it could be inferred that the commercial mullite powder comes from a synthesis process in which the total conversion of the starting mixture (ammonium alum and silica) was not achieved.[11]

The mullite powder presented a bimodal particle size distribution (Mastersizer S, Malvern Instruments, Malvern, UK) with a low mean volume diameter (D_{50} = 1.5 μm), a high volume percentage (~30%) of fine particles <1 μm, and contained agglomerates up to 50 μm in size due to the presence of the very fine particles. These results are consistent with the high value of the specific surface area (13.5 m^2/g) determined by the BET method (Monosorb, Quantachrome Instruments, Boynton Beach, FL, USA). Moreover, it was previously determined[9] that the mullite powder consists of very small three-dimensional particles, some of them faceted, with equiaxial morphology, as well as agglomerates of the smallest particles, which is in agreement with the granulometric distribution.

Commercial native starches (AVEBE Argentina, Buenos Aires, Argentina) derived from cassava, corn, and potato (Table 1), were also used as raw materials. Real densities and total lipid content were determined by He-pycnometry (Multipycnometer, Quantachrome Instruments) and the Soxhlet extraction method, respectively. The values obtained for these parameters were in the range of the values reported for these types of starch.[12] Based on the X-ray diffraction peak positions (X'Pert PRO, PANalytical), the cassava and corn starches were identified as A-type (15.2, 17.1, 18.0, and 22.9°2θ), whereas the potato starch was identified as B-type (5.4, 15.0, 17.2, 21.8, and 24.0°2θ).

The particle size distributions were analyzed (Mastersizer S, Malvern Instruments) using stabilized aqueous starch suspensions. The three starches presented bimodal granulometric distributions with a low volume percentage (<5%) of small granules, which can be linked to impurities or broken granules. The moisture weight percentage was determined by thermogravimetric analysis (TGA; TGA-50, Shimadzu, Kyoto, Japan) at 10 °C/min up to 700 °C, in air. Starch transition temperatures were determined by differential scanning calorimetry (DSC; DSC-50, Shimadzu, Kyoto, Japan) at 5 °C/min up to 120 °C. The granule morphology analysis of the dry starches was performed by scanning electron microscopy (SEM; JSM-6460, JEOL, Tokyo, Japan). Potato starch exhibited the largest granules, with smooth surfaces and oval or spherical forms. Corn and cassava starches presented granules with polyhedral form, but the corn starch granules were the most representative of this type.

2.2. Forming and characterization of green bodies

Based on previously selected experimental conditions, aqueous mullite–starch suspensions (40 vol% total solid loading) were prepared by: (a) mixing mullite powder in water to a solid content of 40 vol% and dispersing with 0.45 wt% Dolapix CE-64 (Zschimmer & Schwarz, Lahnstein, Germany) with respect to the powder amount; (b) homogenizing in a ball mill for 6 h; and (c) adding a volume of aqueous starch suspension (40 vol%) and mixing for 5 min to obtain a final starch and mullite content of 10 vol% and 30 vol%, respectively.

Two novel routes for forming aqueous mullite suspensions with native starches, which were proposed as alternative routes to the conventional route, were designed with the aim of developing green bodies without deformation and with homogeneous porous microstructures.

With the "Sub-gelatinization Route" (SGR) (this route was also called "Pre-gelling Route"),[9] aqueous mullite–starch suspensions were heated at temperatures lower than the onset temperature of gelatinization for each system (59 °C for mullite–cassava starch and mullite–potato starch suspensions, and 64 °C for mullite–corn starch suspension). The temperatures used are the maximum possible temperatures at which each mullite–starch system can be heated without the formation

Table 1
Characteristics of the commercial native starches.

Starch	ρ_r (g/cm^3)	Lipid content (wt%)	D_{50} (μm)	Moisture content (wt%)	T_p (°C)
Cassava	1.49	0.99	13.6	11.5	67.5
Corn	1.49	1.63	14.8	10.9	66.8
Potato	1.47	0.37	47.8	14.4	65.0

ρ_r, real density; D_{50}, mean volume diameter; T_p, endothermic peak temperature.

of gel throughout its volume. These temperatures, referred to as "sub-gelatinization temperatures" in this study, were experimentally determined by heating 20 ml of each mullite–starch suspension on a stirring hot plate equipped with a temperature sensor (±0.1 °C). The heating of the suspension up to the sub-gelatinization temperature was proposed with the following objectives: (a) to cause some granules to reach an incipient state of gelatinization in order to activate the global gelatinization process at the moment the necessary temperature is reached for this to occur, and (b) to decrease the required time to achieve a uniform consolidation temperature throughout the total volume of suspension and, therefore, to minimize not only possible thermal gradients in the sample (thermal gradients can produce microstructural inhomogeneity and defects caused mainly by differential volumetric shrinkage), but also the segregation of mullite particles and starch granules caused by their very different densities and particle sizes.

Based on the above-mentioned premise (to develop porous green bodies with homogeneous microstructures, particularly with regard to the distribution of raw materials and pores), and with the aim of increasing the viscosity of mullite–starch suspensions and, consequently, preventing the segregation of mullite particles and starch granules, another alternative route designated as the "Mixing Route" (MR) was also proposed. With this route, a mixture of ungelatinized native starch and the same type of starch previously gelatinized (10 vol% starch in water, 80 °C for 10 min) was used in order to prepare the aqueous mullite–starch suspensions. The ratio of gelatinized to total starches was 1:10.

The shear flow properties of aqueous mullite–starch suspensions used for each route (SGR and MR) were analyzed by measuring viscosity (HAAKE RS 50, Thermo Electron, Karlsruhe, Germany) using a double-cone/plate sensor configuration (HAAKE DC 60/2°, Thermo Electron, Karlsruhe, Germany). Flow curves were obtained using a three-stage measuring program with a linear increase in shear rate from 0 to 1000 s^{-1} in 300 s, 60 s at 1000 s^{-1}, and further decreasing to zero shear rate in 300 s.

In both routes, mullite–starch disks before the burning-out process (labeled as SGR_{bb} and MR_{bb}) were formed by pouring the aqueous mullite–starch suspension at room temperature into stainless steel cylindrical molds (diameter = 2.20 cm; height = 1.00 cm) covered on the inside with adhesive PTFE (polytetrafluoroethylene, Teflon) tape to facilitate the removal of the samples and prevent the generation of defects due to deficient wetness, and then heating them in an electric stove (UFP 400, Memmert, Schwabach, Germany) at 80 °C for 2 h. Once the consolidation was finished, the samples were taken out of their molds and dried at 40 °C for 24 h.

The densities (ρ) of the bodies were determined by immersion in Hg, and porosities (%P) were calculated from $100\cdot(1-\rho/\rho_p)$. For SGR_{bb} and MR_{bb}, ρ_p was the density of the powdered mixture of mullite and starch determined by He-pycnometry (Multipycnometer, Quantachrome Instruments). Microstructural analysis of the green materials was performed by SEM (JSM-6460, JEOL) on fracture surfaces of the disks.

2.3. Burning-out process and characterization of burned disks

Burned mullite bodies were obtained by burning out the starch at a heating rate of 1 °C/min up to 650 °C for 2 h in an electric furnace with SiC heater elements. The calcining temperature was selected based on the results obtained from TGA (TGA-50, Shimadzu; at 10 °C/min up to 700 °C, in air) of the native starches used as raw materials. This temperature was considered the temperature at which all the organic components (starches and organic additives) were completely removed. Furthermore, to evaluate the effective removal of the starch from the green compacts by the burning-out process, thermogravimetric tests were performed on the mullite–starch (1 °C/min up to 650 °C, 2 h) and burned samples (10 °C/min up to 700 °C). In all the TGA tests, a very low heating rate (1 °C/min) was used to minimize the generation of defects in the green bodies or their rupture during the burnout process due to the evolution of a high volume of gas (particularly water vapor and carbon dioxide) caused mainly by the oxidative degradation of the starch.

From the TGA tests of starch samples, the following percent weight losses were determined: 12.7 wt% up to 150 °C, which is attributed to the removal of the water physically adsorbed onto the surface of the starch granules; 61.2 wt% between 250 °C and 350 °C and 26.1 wt% in the range 350–550 °C, which was associated with the elimination of starch by the thermal and oxidative degradation of the polymeric chains of its structure. After 550 °C, no additional weight loss was recorded. Therefore, a temperature of at least 600 °C was required to remove the starch completely (no starch residue was found in any case). As for the TGA tests of mullite–starch samples, the percent weight losses registered for cassava, corn, and potato starches—assuming that all the organic dispersant was completely removed—were 11.9%, 12.9%, and 9.3%, respectively.

The densities (ρ) of the disks obtained after the burning-out process (SGR_{ab} and MR_{ab}) were determined by Archimedes method (immersion in Hg), and porosities ($\%P$) were calculated from $100\cdot(1-\rho/\rho_p)$. For these samples, ρ_p was the pycnometric density value of the as-received mullite powder. The microstructure of the burned materials was analyzed by SEM (JSM-6460, JEOL) on fracture surfaces.

2.4. Sintering and characterization of porous mullite bodies

The evolution of phases obtained in samples by thermal treatment at different temperatures (1400, 1500 and 1650 °C, for 2 h) was studied by XRD analysis (X'Pert PRO, PANalytical; radiation of CuKα at 40 mA and 40 kV). The different thermal treatments were carried out in an electric furnace with $MoSi_2$ heater elements (RHF 17/6S, Carbolite, Hope Valley, UK). Samples were heated up to the corresponding maximum temperature at 5 °C/min and subsequently cooled to room temperature at 5 °C/min. The weight percentage of α-alumina present in samples treated at the different temperatures was estimated by XRD analysis employing the external standard method[13] for which a standard alumina powder calcined at 1500 °C for 2 h was used. XRD patterns between 42.5°2θ and 44.5°2θ were obtained in experimental conditions with the equipment previously mentioned. For each sample, the average value of the α-Al_2O_3 weight percentage at each treatment temperature was determined by measuring the area of the peak located at 43.4°2θ (distance among crystallographic planes, $d = 2.085$ Å) corresponding to the 113 plane. The diffraction peak selected is the peak of maximum intensity of α-Al_2O_3 (JCPDS File 82-1399).

The maximum sintering temperature (1650 °C) and the employed time (2 h) were selected in order to achieve high densification in the mullite matrix. For this selection, sintering conditions habitually employed for mullite materials[14] and the reported results of dilatometry tests[7] on samples of a commercial mullite powder with physical and chemical properties (purity, mean particle size, composition) similar to those of the mullite powder used in this study were considered. In addition, from the density values measured in disks treated at 1650 °C for 6 h, and assuming that the densification of green bodies is attributed to the removal of interstitial pores, a sintering time longer than that employed (2 h) did not change the degree of matrix densification (disks sintered at 1650 °C for 2 h presented 43% porosity and disks sintered at the same temperature for 6 h achieved 42% porosity). Thus, 2 h at the considered temperatures were considered sufficient.

Bulk densities (ρ_s) and open porosities ($\%P_o$) were determined by the Archimedes method in water, taking into account an error equal to the Hg-immersion method. Total porosities ($\%P_s$) were calculated from $100\cdot(1-\rho_s/\rho_{ps})$, where ρ_{ps} was the density of the powdered sample treated at 1400, 1500 or 1650 °C for 2 h, determined by He-pycnometry. Closed porosities ($\%P_c$) were obtained from the difference between $\%P_o$ and $\%P_s$. The linear and volumetric shrinkage of sintered samples were calculated by using disk geometrical dimensions measured with a slide caliper (Starrett Company, Athol, MA). The final microstructures were analyzed by SEM on the fracture surfaces of disks. The mean size and morphology of the cavities and the grains were determined together with the degree of pore connectivity (defined as the open porosity/total porosity ratio). Mercury porosimetry (AutoPore II 9215; Micromeritics, Aachen, Germany) was used to determine the pore throat size distributions in the materials sintered at 1500 and 1650 °C for 2 h.

3. Results and discussion

3.1. Shear flow properties of aqueous mullite–starch suspensions used in the SGR and MR

The flow properties of aqueous mullite–starch suspensions used in the SGR, measured at 59 °C when cassava and potato starches were used and at 64 °C in the case of corn starch, as well as the flow properties of the suspensions used in the MR, measured at room temperature, were evaluated. Rheological testing thus determined that, in the first case, the viscosity of the suspensions did not increase with respect to the viscosity of those prepared at room temperature. This result can be explained considering that only some of the granules of each system were gelatinized at the corresponding temperatures used; in consequence, the formation of a three-dimensional gel structure did not occur in either system. However, when a small amount of non-gelatinized native starch was replaced by the same type of starch previously gelatinized (aqueous mullite–starch suspensions used to shape green disks by MR), the apparent viscosity (η_{1000}) notably increased by at least six times in every case (Table 2).

Moreover, the viscosity values obtained were in the range of the values reported for systems that use a chemically modified starch (TRECOMEX AET1), as reported by Barea et al.

Table 2
Apparent viscosity at 1000 s^{-1} (η_{1000}) of aqueous mullite–starch suspensions.

Aqueous suspensions	Mullite content (vol%)	Non-gelatinized starch content (vol%)	Gelatinized starch content (vol%)	η_{1000} (mPa s)
Mullite–cassava	30	10	0	21
Mullite–cassava in MR	30	9	1	156
Mullite–corn	30	10	0	19
Mullite–corn in MR	30	9	1	116
Mullite–potato	30	10	0	16
Mullite–potato in MR	30	9	1	183

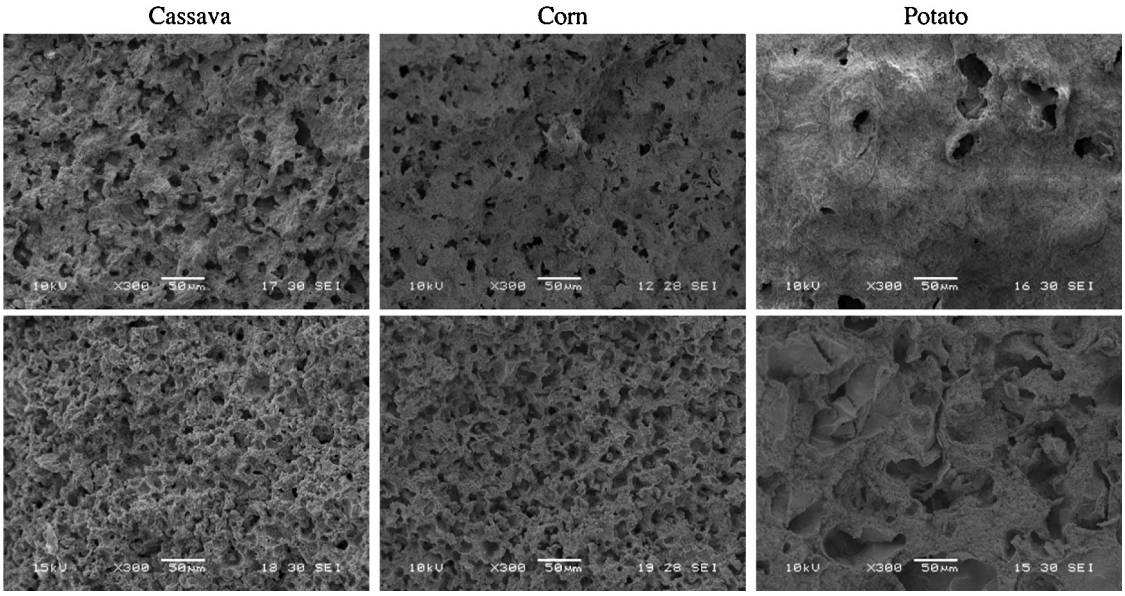

Fig. 1. SEM micrographs of the fracture surface of SGR_{bb} (top) and SGR_{ab} (bottom).

The presence of the three-dimensional structure of starch gel and its water uptake capacity are the factors that could explain the increase recorded in the viscosity. Thus, the higher viscosity presented by the mullite–potato starch suspension with gelatinized starch could be related to the greater water uptake capacity shown by this starch. It is well known that the water-retention capacity depends on the concentration of and structure formed by the amylose and amylopectin molecules in the gel, the degree and length of their branches, and the presence of other components, such as lipids and phosphate groups,[15,16] and therefore of the type of starch. In this work, the water-retention capacity (WRC), calculated as the ratio of the mass of water in the gel and the initial mass of the starch, was determined using a modification of the methods reported by Bryant and Hamaker.[17] For the WRC measurements of each starch, 1 g of sample and 10 ml of water were placed in a centrifuge tube. The tubes were heated and stirred for 10 min in water bath at 80 °C. They were then cooled to room temperature and centrifuged at 1000 × *g* for 15 min, and the supernatant liquid was removed and weighed. Finally, the mass of water in the gel was calculated by subtracting the initial mass of water from the mass of the supernatant liquid. The gels developed in these conditions were shown to have the following values for WRC: 6.7 for cassava starch, 5.4 for corn starch, and 7.9 for potato starch.

3.2. Characterization of green and burned bodies

Disks obtained before the burning-out process (SGR_{bb} and MR_{bb}) achieved a mean diameter of 2.17 ± 0.01 cm, a height of 0.55 ± 0.05 cm and shrinkage of 1.3% in diameter and 8.3% in height. Mullite disks obtained after calcination (SGR_{ab} and MR_{ab}) maintained the mentioned dimensions without displaying cracks or deformations.

High porosities were achieved in all the green materials. The type of forming route and starch used did not lead to significant differences in porosity values for any disk obtained before the burning-out process ($\%P_{bb} = 56 \pm 2$). For all obtained materials, the porosity of disks notably increased after the burning-out process ($\%P_{ab} = 69 \pm 1$). These values turned out to be consistent with those calculated (~69%) assuming that the totality of the added starch was removed during this process. This result would indicate that there was no segregation of starch granules and mullite particles.

Typical SEM images of the fracture surfaces of materials prepared by both consolidation routes, before and after the burning-out process, are shown in Figs. 1 and 2.

In the images corresponding to SGR_{bb} and MR_{bb}, a homogeneous distribution of raw materials can be observed, which confirms that there was no segregation in any case. In all the materials (Figs. 1 and 2), similar porosities can be seen, which is in agreement with the porosity values determined by density measurements. The porosity of SGR_{bb} and MR_{bb} was associated with highly tortuous cavities throughout the entire thickness of the disks, which hindered the accurate measurement of their size. However, it can be observed that in every sample, the cavity sizes correspond to those of the dry starch granules or those with a certain degree of swelling.

On the other hand, in every green microstructure, except for the fracture surface of the disk prepared by the Mixing Route using potato starch, granules with integrity were not observed. This result can be associated with an advanced gelatinization process occurring that consequently encouraged the loss of granular integrity. However, in the microstructure of the material obtained with the potato starch (Fig. 2), granules that preserved their integrity were observed. The high water uptake capacity of the potato starch decreased the available water volume, and in consequence, prevented the gelatinization of all the granules.

After the burning-out process, the porosity of all the materials (SGR_{ab} and MR_{ab}) (Figs. 1 and 2) notably increased while maintaining the tortuous morphology of the cavities.

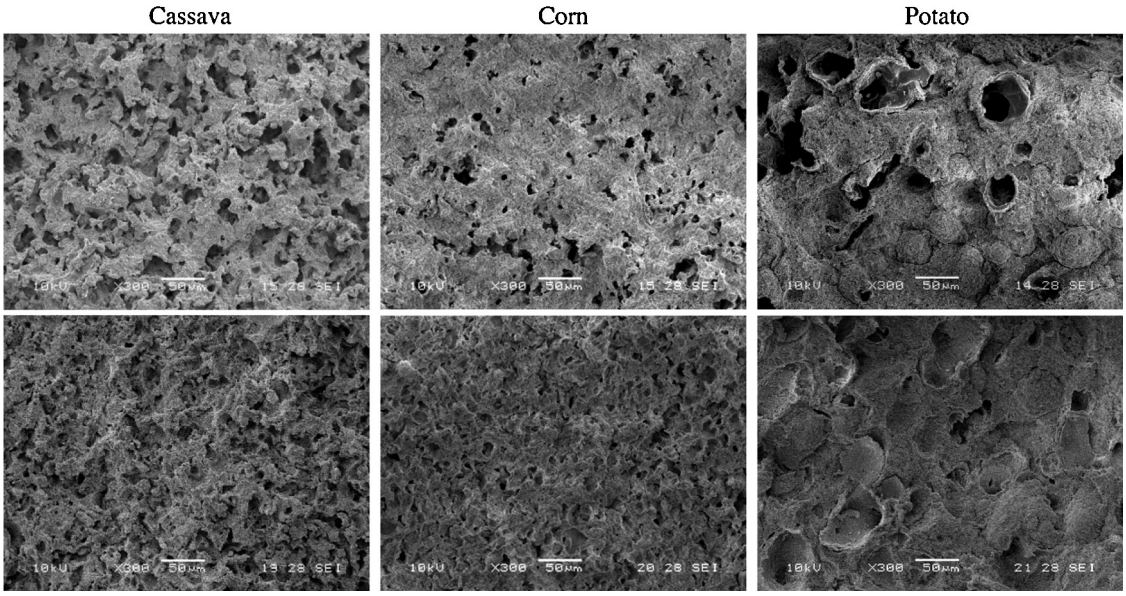

Fig. 2. SEM micrographs of the fracture surface of MR_{bb} (top) and MR_{ab} (bottom).

3.3. Sintering and characterization of porous mullite bodies

XRD patterns of commercial mullite powder, together with those of powdered samples treated at 1400, 1500 and 1650 °C for 2 h, are shown in Fig. 3.

Fig. 4 shows the XRD patterns used to determine the weight percentage of α-alumina presents in the commercial mullite powder and in the samples treated at each temperature employing the external standard method.

As previously mentioned, the presence of θ-alumina—which is a metastable phase—and the medium crystallinity of the as-received mullite powder enable us to conclude that the commercial mullite comes from an incomplete synthesis process.

Based on the XRD pattern of the sample treated at 1400 °C, the mullite peaks were narrower and higher than those corresponding to the as-received mullite powder. Moreover, the peaks corresponding to θ-alumina were not detected, and the intensity of α-alumina peaks increased (Fig. 3), which is in agreement with the results obtained by quantitative analysis; the amount of α-alumina increased from 5.6% to 20.3%. Both results indicate the transformation of θ-alumina to the thermodynamically stable phase (α-alumina). A small degree of mullitization due to a reaction between some of the sources of Al_2O_3 and SiO_2 cannot be ruled out. In addition, the diffraction peak at 21.8°2θ corresponding to the main peak of the cristobalite phase increased in intensity and was narrower than the peak present in the pattern of the original sample, while the band assigned to the non-crystalline siliceous phases decreased. These results can be associated with an increase of the crystallinity of the phases, although the transformation of non-crystalline siliceous phases to cristobalite cannot be ruled out. Moreover, the increase in pycnometric density registered in the material treated at 1400 °C (3.16 g/cm^3) with respect to the original mullite powder (3.07 g/cm^3) is evidence of the transformation of θ-alumina ($\rho = 3.28$ g/cm^3) to α-Al_2O_3 ($\rho = 3.98$ g/cm^3) and even the mullite formation ($\rho = 3.16$ g/cm^3).

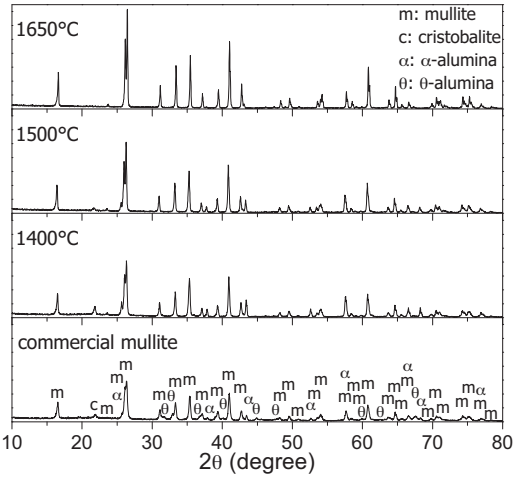

Fig. 3. XRD patterns of as-received mullite powder and mullite powdered samples treated at 1400, 1500 and 1650 °C, 2 h.

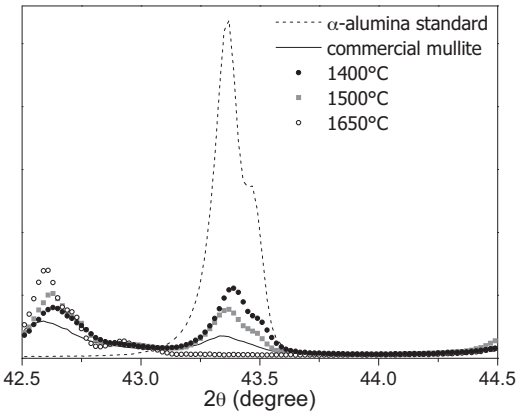

Fig. 4. XRD patterns of α-alumina powder used as an external standard, commercial mullite powder and mullite powdered samples treated at different temperatures.

Table 3
Total ($\%P_s$), open ($\%P_o$) and closed ($\%P_c$) porosity values, degree of pore connectivity, and linear and volumetric shrinkage of sintered disks.

Forming route	Starting system	Temp. (°C)	$\%P_s$	$\%P_o$	$\%P_c$	Pore connectivity degree	Linear shrinkage (%)	Volumetric shrinkage (%)
SGR	Mullite–cassava	1400	63	62	0.7	0.98	3.2 ± 0.3	9.5 ± 0.5
		1500	56	55	1.0	0.98	8.1 ± 0.1	22.4 ± 0.2
		1650	44	42	2.0	0.95	16.1 ± 0.6	40.5 ± 0.9
	Mullite–corn	1400	63	62	1.1	0.98	2.2 ± 0.1	6.6 ± 0.2
		1500	55	53	1.9	0.96	7.8 ± 0.1	21.6 ± 0.2
		1650	43	39	3.6	0.91	16.9 ± 0.2	40.5 ± 0.3
	Mullite–potato	1400	62	60	1.5	0.97	2.8 ± 0.3	8.4 ± 0.5
		1500	54	52	1.9	0.96	8.1 ± 0.1	22.3 ± 0.2
		1650	43	38	4.7	0.88	16.9 ± 0.8	43 ± 1
MR	Mullite–cassava	1400	63	62	0.7	0.98	3.4 ± 0.6	9.6 ± 0.9
		1500	55	54	1.2	0.98	8.1 ± 0.4	22.2 ± 0.6
		1650	42	40	2.4	0.95	15.6 ± 0.8	41 ± 1
	Mullite–corn	1400	61	60	0.8	0.98	3.5 ± 0.3	9.9 ± 0.5
		1500	53	51	1.8	0.96	8.3 ± 0.1	23.0 ± 0.2
		1650	39	35	4.2	0.90	16.1 ± 0.2	42.8 ± 0.3
	Mullite–potato	1400	64	63	1.1	0.98	3.3 ± 0.4	8.3 ± 0.6
		1500	55	53	2.4	0.96	8.2 ± 0.2	22.8 ± 0.3
		1650	40	35	5.2	0.87	16.5 ± 0.6	41.8 ± 0.9

At 1500 °C, mullite diffraction peaks were even more intense, while the intensity of α-Al_2O_3, the cristobalite peaks and the band assigned to non-crystalline phases decreased. The weight percentage of α-Al_2O_3 in the sample treated at this temperature was 12.8%. Thus, the results indicate a certain degree of reaction between α-Al_2O_3 and the SiO_2 sources to give mullite. In this case, the pycnometric density of the treated powder at 1500 °C ($\rho = 3.15$ g/cm^3) was similar to the value determined for the powder treated at 1400 °C.

At 1650 °C, only the characteristic mullite diffraction peaks with intensities much higher than those of the peaks present in the sample treated at 1500 °C were observed. A complete mullitization reaction at 1650 °C was assumed to have occurred (the density of the powder treated at 1650 °C was 3.11 g/cm^3).

Total, open and closed porosity values, together with the degree of pore connectivity and shrinkage values of mullite disks obtained after sintering, are given in Table 3.

The total porosity values of disks consolidated by both routes were similar for all the starches used, and decreased when the treatment temperature increased (61–64% at 1400 °C, 53–56% at 1500 °C, and 39–44% at 1650 °C). In addition, the open porosity decreased when the temperature increased (60–63% at 1400 °C, 51–55% at 1500 °C, and 35–42% at 1650 °C), with the consequent increase of the closed porosity (0.7–1.5% at 1400 °C, 1.0–2.4% at 1500 °C, and 2.0–5.2% at 1650 °C), which is in agreement with the classic theory of sintering in which interstitial concave pores forming an open network are closed in the last steps of the sintering process. For both the linear and volumetric shrinkage of mullite disks, the obtained values were in the range of those reported for bodies consolidated by the conventional route with a waxy corn starch.[18,19] As for the degree of connectivity, the ranking for samples obtained at 1650 °C with the different starting systems was mullite–cassava > mullite–corn > mullite–potato starches. This order could be related to the characteristics of the green microstructures derived from the gel formation process. During this process, a mixture is formed of swollen granules and granule fragments immersed in a colloidal dispersion of starch components (i.e. the gel) with characteristics dependent on the botanical source of the starch. Thus, this three-dimensional gel, which includes a varying amount of ceramic particles depending on the starch type, gives rise to structures with different degrees of interconnection.

The obtained porosity values were in the range of those reported for porous mullite materials prepared by the conventional route with a similar percentage of modified starch.[7] It is well-known that total porosities achieved in the materials prepared by SCC do not correspond directly to the nominal starch content in the suspension, but they are significantly higher due to the swelling experienced by the starch granules during the thermal consolidation process. However, despite the fact that swelling capacity depends on the starch type, the total porosity of the disks did not significantly vary with the native starch type, which is the same as what occurred in the green bodies and which is in agreement with what happens with constrained swelling due to steric effects (excluded volume effect).

Taking into account that the sintering temperature is the main factor determining the matrix porosity and that large pores (bigger than the grain size) embedded in a ceramic matrix with small pores does not significantly contribute to the shrinkage of the body, the recorded shrinkage in all the mullite disks was assumed to correspond essentially to the matrix. Based on the linear and volumetric shrinkage percentages, which were similar for the three native starches, and assuming that this shrinkage occurs only in the ceramic matrix, it can be inferred that the packing density of the mullite particles in every green body is approximately the same.

Materials obtained at 1400 °C, regardless of the consolidation route and starch type used, presented microstructures with elevated porosity and scarce development of solid necks into

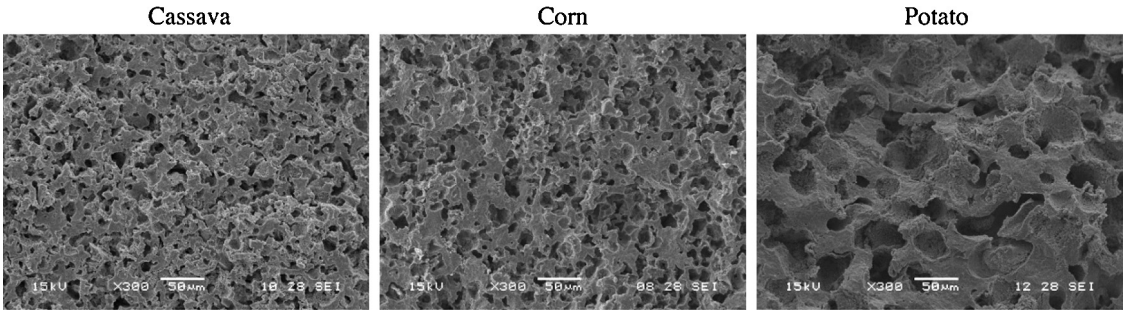

Fig. 5. SEM micrographs of fracture surfaces of the disks formed by SGR, after sintering at 1650 °C.

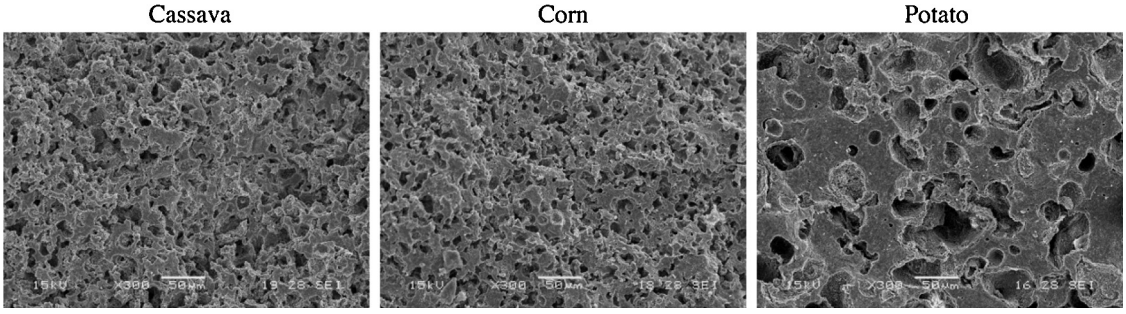

Fig. 6. SEM micrographs of fracture surfaces of the disks formed by MR, after sintering at 1650 °C.

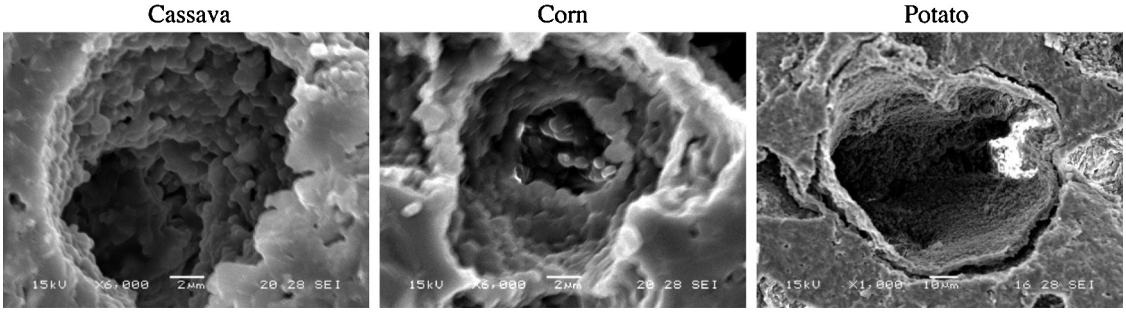

Fig. 7. SEM images of typical cavities developed in the materials at 1650 °C.

the matrix, which indicates a low cohesion of particles and a low degree of sintering. At 1500 °C, the sintering of the mullite matrix increased considerably by decreasing its porosity and forming solid necks. For both temperatures, the porosity was associated with the presence of large cavities whose size depended on the starch type used (10–20 μm for materials prepared with native starches of cassava and corn, and 30–70 μm for those prepared with potato starch), and much smaller interstitial pores in the ceramic matrix.

Typical SEM images of materials sintered at 1650 °C and prepared with the three starches using SGR and MR are shown in Figs. 5 and 6, respectively. In Fig. 7, SEM images with a higher magnification of the typical cavities developed with each starch are shown.

Large convex cavities (cells) embedded in the mullite matrix were created by the removal of native starch granules, and much smaller pore channels or throats (cell windows) interconnecting these cavities were developed after the sintering treatment. As what occurred at the other temperatures, at 1650 °C, cavity size was mainly determined by the native starch type and

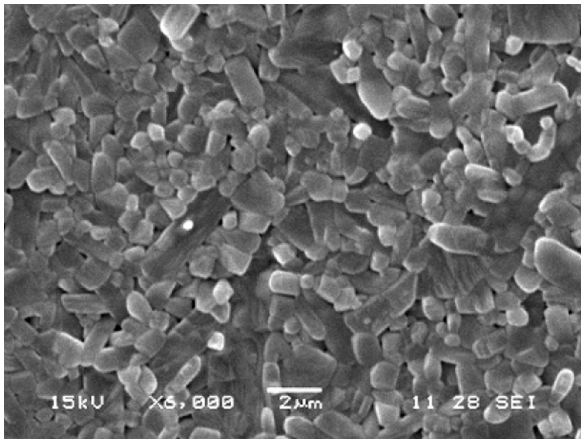

Fig. 8. Typical SEM micrograph of the mullite matrix of a disk sintered at 1650 °C.

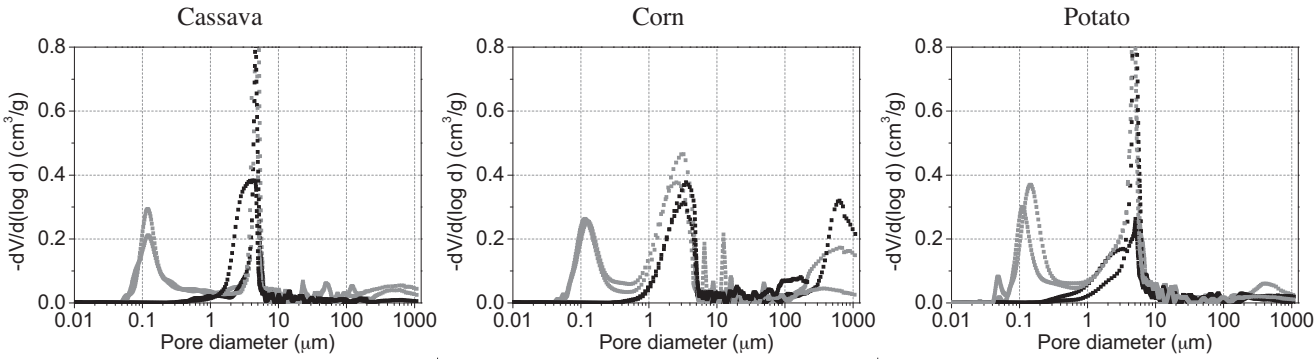

Fig. 9. Pore size distributions obtained by Hg-porosimeter. Lines: gray for 1500 °C and black for 1650 °C.

was related to dry starch granule sizes or those having suffered some degree of swelling. The mean cavity sizes were similar to those determined in the materials sintered at 1500 °C. Larger cavities generated by the joining of various cavities were also observed. In the material prepared with potato starch by both routes, cavities with a shell and circumferential cracks in the cavity/matrix interface were observed by SEM, as reported in previous research.[8]

The mullite matrix (Fig. 8) displayed a high degree of densification furthered by the presence of phases based on silicates with low melting points. It is constituted of submicronic grains (some of which were generated by the mullitization reaction at high temperature), mainly equiaxial (∼0.5 μm), together with other slightly larger grains with an elongated morphology (maximum length and width of 2 μm and 0.8 μm, respectively, and "aspect ratio" < 2.5) whose development is related to their growth in the presence of the liquid phase.

For sintering temperatures of 1500 and 1650 °C, the pore sizes measured in all the materials by mercury porosimetry (Fig. 9) were much lower than the cavity sizes determined by SEM, as was expected based on the characteristics of the developed pores: large cavities interconnected by pore channels or throats of much lower size. This result can be attributed to the "bottle neck" effect that occurs when the mercury accesses a large cavity through a narrow channel. In this manner, the pore diameters determined by mercury porosimetry corresponded to the pore throat diameters. According to these results, the pore throat size distributions for the materials prepared with each of the starches were similar so that again, there was no dependence on the forming route used.

The porous materials sintered at 1500 °C exhibited bimodal pore size distributions due to the partial densification of the matrix in these materials. In this case, there are two different populations, one of which corresponds to the interconnections between cavities (cell windows), and the other to the much smaller interstitial open pores. For the first distribution, the determined pore sizes were the following: 3.7–5.8 μm, 1.3–4.6 μm and 3.0–6.4 μm, for the materials prepared with cassava, corn and potato starches, respectively. Thus, the pore throat diameters varied slightly with the starch type used: materials prepared with potato starch presented diameters slightly larger than those determined for the materials obtained with cassava starch, and even more so compared with those generated in the materials consolidated with corn starch. For the materials prepared with potato starch as those with corn starch, the corresponding interval of sizes was equally greater than that determined for the material obtained with cassava starch. On the other hand, the interstitial pore sizes were similar in every material: 0.09–0.15 μm, 0.09–0.16 μm and 0.09–0.18 μm, for the materials prepared with cassava, corn and potato starches, respectively. Results reported by other authors for materials prepared by the conventional route (SCC)[19] indicate that the sizes for both populations of pores did not depend on the starch type used.

In the pore size distributions corresponding to the materials sintered at 1650 °C, the population assigned to the pores of the ceramic matrix was not observed, which is in agreement with the fact that the matrix achieved a high densification degree at this temperature. The pore throat diameters for the materials prepared with cassava, corn, and potato starches and treated at 1500 and 1650 °C were in the ranges 3.3–5.4 μm, 1.8–4.9 μm, and 3.6–6.3 μm, respectively, which indicates that the temperature did not significantly modify the range of sizes; only in some cases were the distributions slightly narrower, while in other cases they did not change their amplitude.

4. Conclusions

Highly porous mullite green bodies without cracks or deformation and with homogeneous microstructures were formed by using the proposed processing routes. In this way, the segregation of starch granules and mullite particles, previously observed in bodies formed by the conventional route, was prevented, and a homogeneous distribution of raw materials was achieved in each green material.

From the study of the evolution of the material as a function of temperature, it was determined that the transformation of θ-alumina to α-alumina occurred at 1400 °C as well as a certain amount of reaction between α-Al_2O_3 and the SiO_2 sources to give mullite at 1500 °C, although a small degree of mullitization due to the reaction between some of the sources of Al_2O_3 and SiO_2 could have already occurred at lower temperature. Complete mullitization was also determined to have taken place at 1650 °C.

A high total porosity was developed in all materials sintered at the highest temperatures used (i.e. 1500 and 1650 °C). Similar

porosity values were obtained at each temperature independently of the starch type used. This porosity was always associated with large highly interconnected non-spherical cavities, whose sizes depended on the starch type, and much smaller size pore throats interconnecting these cavities. In particular, the materials treated at 1500 °C showed interstitial open pores, whereas the population assigned to these pores was not determined in those materials sintered at 1650 °C, indicating that a high degree of densification of the matrix occurred, which was furthered by the presence of phases based on silicates with low melting points. In all materials sintered at 1650 °C, the matrix was constituted of submicronic mullite grains with a mainly equiaxial and elongated morphology.

Acknowledgements

The authors gratefully acknowledge Prof. Dr. R. Moreno (Institute of Ceramics and Glass, CSIC, Madrid, Spain) for carrying out the measurements of Hg-porosimetry, and Dr. M.I. Nieto and Ms. S. Benito of the same institute for accomplishing the measurements of laser diffraction, pycnometric densities, and particle size distributions of the starches used in this work. This study was funded by CONICET (Argentina) under project PIP 0936.

References

1. Schneider H, Schreuer J, Hildmann B. Structure and properties of mullite – a review. *J Eur Ceram Soc* 2008;**28**(2):329–44.
2. Hildmann B, Schneider H. Heat capacity of mullite – new data and evidence for a high-temperature phase transformation. *J Am Ceram Soc* 2004;**87**(2):227–34.
3. Schneider H, Eberhard E. Thermal expansion of mullite. *J Am Ceram Soc* 1990;**73**(67):2073–6.
4. She JH, Ohji T. Fabrication and characterization of highly porous mullite ceramics. *Mater Chem Phys* 2003;**80**(3):610–4.
5. Lyckfeldt O, Ferreira JMF. Processing of porous ceramics by 'starch consolidation'. *J Eur Ceram Soc* 1998;**18**(2):131–40.
6. Alves HM, Tarì G, Fonseca AT, Ferreira JMF. Processing of porous cordierite bodies by starch consolidation. *Mater Res Bull* 1998;**33**(10):1439–48.
7. Barea R, Osendi MI, Miranzo P, Ferreira JMF. Fabrication of highly porous mullite materials. *J Am Ceram Soc* 2005;**88**(3):777–9.
8. Talou MH, Moreno R, Camerucci MA. Porous mullite ceramics formed by direct consolidation using native and granular cold-water-soluble starches. *J Am Ceram Soc* 2014;**97**(4):1074–82.
9. Talou MH, Camerucci MA. Two alternative routes for starch consolidation of mullite green bodies. *J Eur Ceram Soc* 2010;**30**(14):2881–7.
10. Camerucci MA [Ph.D. thesis] *Development and evaluation of cordierite and cordierite–mullite ceramic materials*. Mar del Plata (ARG): National University of Mar del Plata; 1999.
11. Wojciechowska R, Wojciechowski W, Kaminski J. Thermal decompositions of ammonium and potassium alums. *J Therm Anal Calorim* 1988;**33**(2):503–9.
12. Jane J. Structural features of starch granules II. In: BeMiller JN, Whistler RL, editors. *Starch: chemistry and technology*. New York: Academic Press; 2009. p. 193–236.
13. Cullity BD, Stock SR. *Elements of X-ray diffraction*. 3rd ed. New Jersey: Prentice Hall; 2001.
14. Sacks MD, Lee HW, Pask JA. A review of powder preparation methods and densification procedures for fabricating high density mullite. In: Somiya S, Davies RF, Pask JA, editors. *Ceramic transactions*, vol. 6. Westerville, OH: American Ceramic Society; 1990. p. 167–207.
15. Hoover R. Composition, molecular structure, and physicochemical properties of tuber and root starches: a review. *Carbohydr Polym* 2001;**45**(3):253–67.
16. Singh N, Singh J, Kaur L, Sodhi NS, Gill BS. Morphological, thermal and rheological properties of starches from different botanical sources. *Food Chem* 2003;**81**(2):219–31.
17. Bryant CM, Hamaker BR. Effect of lime on gelatinization of corn flour and starch. *Cereal Chem* 1997;**74**(2):171–5.
18. Gregorová E, Pabst W, Bohačenko I. Characterization of different starch types for their application in ceramic processing. *J Eur Ceram Soc* 2006;**26**(8):1301–9.
19. Pabst W, Gregorová E, Sedlářová I, Černý M. Preparation and characterization of porous alumina–zirconia composite ceramics. *J Eur Ceram Soc* 2011;**31**(14):2721–31.